Accepted Manuscript

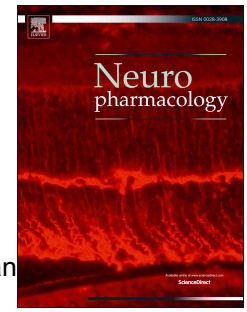

PPARβ/δ activation protects against corticosterone-induced ER stress in astrocytes by inhibiting the CpG hypermethylation of MicroRNA-181a

Juan Ji, Xiao-Ning Zeng, Lu-Lu Cao, Ling Zhang, Zhan Zhao, Dan-Dan Yang, Xiu-Lan Sun

PII: S0028-3908(16)30476-2

DOI: 10.1016/j.neuropharm.2016.10.022

Reference: NP 6488

To appear in: *Neuropharmacology*

Received Date: 14 March 2016

Revised Date: 27 September 2016

Accepted Date: 22 October 2016

Please cite this article as: Ji, J., Zeng, X.-N., Cao, L.-L., Zhang, L., Zhao, Z., Yang, D.-D., Sun, X.-L., PPARβ/δ activation protects against corticosterone-induced ER stress in astrocytes by inhibiting the CpG hypermethylation of MicroRNA-181a, *Neuropharmacology* (2016), doi: 10.1016/j.neuropharm.2016.10.022.

PPARβ/δ Activation Protects Against Corticosterone-induced ER Stress in Astrocytes by Inhibiting the CpG Hypermethylation of MicroRNA-181a

Juan Ji[1,3], Xiao-Ning Zeng[2,3], Lu-Lu Cao[1], Ling Zhang[1], Zhan Zhao[1], Dan-Dan Yang[1], Xiu-Lan Sun[1]

1. Jiangsu Key Laboratory of Neurodegeneration, Department of Pharmacology, Nanjing Medical University, 101Longmian Road, Nanjing, Jiangsu 211166, China
2. The first affiliated hospital, Nanjing Medical Universisty, 300 Guangzhou Road, Nanjing, Jiangsu 210029, China
3. The first two authors contributed equally to this work.

Corresponding author:

Prof. Xiu-Lan Sun, M.D., Ph.D.

Jiangsu Key Laboratory of Neurodegeneration

Department of Pharmacology

Nanjing Medical University

101Longmian Road

Nanjing, Jiangsu 211166, China

Tel: 86-25-86862127, Fax: 86-25-86863108

Email: xiulans@njmu.edu.cn

Running title: PPARβ/δ inhibits microRNA181a hypermethylation

Abstract

Increasing evidence indicates that peroxisome proliferator-activated receptors (PPARs) play neuroprotective roles in various neurodegenerative disease models *in vivo* and *in vitro*. However, the underlying mechanisms remain unclear. Astrocyte proliferation is a key process in neural development and plays significant roles in the regeneration of neural tissue after a penetrating injury. Corticosterone can significantly reduce the expression of glial fibrillary acid protein (GFAP) in cultured rat hippocampal astrocytes *in vitro*, and induce astrocytic dysfunction. Our research found that corticosterone treatment resulted in astrocyte damage and reduced the expression of PPARβ/δ. GW0742, a selective and high-affinity PPARβ/δ agonist, attenuated the corticosterone-induced astrocyte damage, but also significantly reversed the increase in the expression of GRP78 and CHOP, the two predominant proteins in endoplasmic reticulum (ER) stress. Moreover, GW0742 decreased the levels of caspase-12 and cleaved caspase-3, thereby protecting astrocytes against corticosterone-induced astrocyte apoptosis. We then confirmed that GRP78 was a target gene of microRNA-181a and found that PPARβ/δ activation increased microRNA-181a levels. Finally, we demonstrated that PPARβ/δ activation by GW0742 noticeably inhibited the activities and expression of DNA methyltransferases, and reduced the corticosterone-induced CpG island hypermethylation of microRNA-181a1 in astrocytes. Therefore, the present study is the first to reveal that PPARβ/δ activation suppresses CpG island hypermethylation-associated silencing of microRNA-181a and thereby protects against ER stress-induced damage in astrocytes. Our findings suggest that PPARβ/δ activation in astrocytes might be a promising target for regulating ER stress-induced astrocytic injury.

Keywords: PPARβ/δ; ER stress; methylation; miR181a; GRP78

1. Introduction

Peroxisome proliferator-activated receptors (PPARs) are ligand-activated transcription factors and members of the nuclear receptor superfamily. Three PPAR isoforms, designated PPARα, PPARβ/δ, and PPARγ, are differentially expressed in several tissues and play important roles in various physiological and pathological processes, such as diabetes and obesity (Heneka et al., 2007; Moreno et al., 2004; Desvergne et al., 1999; Wahli et al., 2012). Furthermore, all PPAR isotypes are expressed in the brain (Heneka et al., 2007). Recently, more and more evidence demonstrates that PPARs are actively involved in the modulation of astrocyte metabolism under brain injuries and neurodegenerative diseases, including depression, ischemic brain injury, Parkinson's disease (PD), Alzheimer's disease (AD), Huntington's disease (HD), multiple sclerosis (MS), and amyotrophic lateral sclerosis (ALS) (Joardar et al., 2015; Mandrekar et al., 2013). However, the physiological functions and mechanisms in modulating astrocyte metabolism of these receptors under brain injuries and neurodegenerative diseases are not well known, especially for PPARβ/δ.

Since astrocytes contribute to about 40–60 % of the cells in the brain (Shaha et al., 2016), it is important to understand their broad roles in the central nervous system (CNS). Astrocytes provide nutrients, redox molecules, glucose, and lactate metabolism for neurons (Pellerin, 2008; Allaman et al., 2011; Wilhelm et al., 2012), maintain extracellular ionic environment homeostasis (Simard et al., 2004; Obara et al., 2008; Rash et al., 2010; Papadopoulos et al., 2013; Sibille et al., 2014), and uptake and release neurotransmitters (Simard et al., 2004; Schousboe et al., 2004; Sattler et al., 2006). Recent studies demonstrated that astrocytes gradually become a target for neuroprotection in some CNS diseases, such as stroke, major depression, and schizophrenia (Banasr et al., 2008; Xia et al., 2014), And astrocyte apoptosis is now considered a key factor in the development of various neurodegenerative diseases since astrocytic apoptosis seriously impairs astrocytic functions (Takuma et al., 2004). Therefore, the investigation of specific molecular mechanisms to inhibit astrocyte

apoptosis might provide novel targets for neuroprotection.

An extensive body of literature reports that prolonged exposure to stress or glucocorticoid (GC) leads to a number of brain disorders, including major depression, dementia, addiction, and schizophrenia (Law et al., 2014; Lussier et al., 2013; Patti et al., 2013). Astrocytes widely express the stress hormone receptors mineralocorticoid and glucocorticoid (MR and GR, respectively). In various studies, reduced astrocyte density and function in the limbic regions of the brain have been associated with stress pathology and glucocorticoid overproduction (Chatterjee et al., 2013; Rajkowska et al., 2007; Czeh et al., 2007). Furthermore, accumulating reports show that persisting exposure to high concentration of corticosterone could cause DNA damage, induce differential protein activation in nerve cells, and consequently lead to neuron apoptosis. Furthermore, although chronic corticosterone stimulation induces astrocytic loss in brain disorders, the mechanism of corticosterone-mediated damage in astrocytes remains unclear.

The endoplasmic reticulum (ER) controls metabolism for eukaryotic cells, and changes in the intracellular environment can lead to ER stress (Gulyaeva, 2015). However, exposure to devastating stress damages ER homeostasis, leading to an adaptive unfolded protein response (UPR) to compensate damage (Ron et al., 2002; Kadowaki et al., 2004; Marciniak et al., 2006; Xu et al., 2005). ER stress has been implicated in several diseases such as PD, ischemia, atherosclerosis, and diabetes (Zhou et al., 2013; Hetz et al., 2013). Primarily, the unfolded protein of the ER had occurred unconventionally stacked in dysfunctioning astrocytes, which illustrates that astrocytic ER stress could affect its function and energy metabolism. ER stress mediated inflammatory pathways and the cell apoptosis pathway, which affected cell growth, differentiation, survival and apoptosis. Thus it played an important role in the development of metabolic disease.

Therefore, the present work established a corticosterone-stimulated astrocytic damage model to explore the effects of activated PPARβ/δ in corticosterone-induced astrocyte apoptosis. Our findings expanded the neuropharmacological action of PPARs and provided a novel strategy to overcome ER stress-mediated apoptosis.

2. Materials and Methods

2.1 Primary Astrocyte Cultures

Confluent primary astrocyte cultures were prepared from 1- to 3-day-old neonatal Sprague-Dawley rats as previously described by Strokin et al. (2004). These rats which were purchased from Shanghai Sippr-Bk Laboratory Animal Co., Ltd. (Shanghai, China). All animal operation procedures were performed in accordance with guidelines from the Institution for Animal Care and Use Committee, and approved by the Jiangsu Province Association of Experimental Animals. Briefly, new born pups were immediately sterilized using 75 % alcohol after decapitation. The skulls were dissected, cerebrums carefully placed on dishes containing sterile cold D-Hank's, and the meninges and blood vessels then separated and removed from the cerebral cortices. All cortex tissue was collected in D-Hank's, which contained 0.25 % trypsin (Gibco, Grand Island, USA), and digested for 20 min at 37 °C. Before filtration through a 136 μm mesh, the cortex digestion was terminated by the addition of Dulbecco's modified Eagle's medium (DMEM; Gibco, Grand Island, USA) supplemented with 10 % fetal bovine serum (FBS; Gibco, Grand Island, USA). Lastly, the cell pellets were resuspended after centrifugation at 1500 rpm for 5 min, and seeded in a poly-D-lysine-coated (0.1 mg/mL; Sigma Chemical, St. Louis, MO, USA) 25 cm^2 culture flask. The cultures were maintained at 37 °C in a humidified 5 % CO_2–95 % air atmosphere. The culture medium was renewed the next day and every 2–3 days afterward. The culture was continued for 10 to 12 days. Before experiments, the percentage of primary astrocytes was confirmed to be greater than 97 % purity using staining for the astrocyte marker glial fibrillary acid protein (GFAP).

2.2 Drugs and Treatment

Corticosterone, which was purchased from Sigma Chemical (St. Louis, MO, USA), was dissolved at 100 mM concentration in dimethylsulfoxide (DMSO; Sigma, St. Louis, Mo, USA) and kept as a stock solution. Next, corticosterone that was diluted to

10 μM concentration (containing a maximum of 0.01 % DMSO) was used for *in vitro* experiments. To determine which receptor was involved, we used the selective PPARβ/δ agonist GW0742 (Selleck Chemical, Houston, USA) and the PPARβ/δ antagonist GSK3787 (Selleck Chemical, Houston, USA). DMSO was added to dissolve each of these compounds at 100 mM concentration, and the solutions were then diluted to a final concentration of 10 μM for experiments (containing a maximum of 0.01 % DMSO). Drug dosages were chosen based on the literature (Guo et al., 2013; Kong et al., 2014; Vittoria et al., 2010; Martin et al., 2013). All cultures were divided into 4 groups: the control group, model group, therapeutic group, and antagonistic group. Only the respective vehicles were used in the controls.

2.3 Cell Viability Assay

The methyl thiazolyl tetrazolium (MTT) assay was used to assess astrocyte viability through formazan formation measurements. Astrocytes were seeded onto 96-well plates at a density of 5×10^4 cells per well. After 24 hours of adherence, the cells were successively treated with different drugs, such as corticosterone and/or GW0742 or GSK3787, and incubated in a CO_2 incubator for 24 hours. Then, 20 μL of MTT at a concentration of 5 mg/mL was added to each well with the medium and incubated for 4 hours at 37 °C. Finally, the medium was removed from the wells, and 150 μL of DMSO was added to dissolve the formazan crystals. The absorbance of the colored solutions was quantified using a spectrophotometer with an excitation wavelength of 570 nm (iMark Microplate Reader; Bio-Rad, Hercules, CA). Cell activity was calculated as a percentage according to the following formula: percentage cell viability = (absorbance of the experiment sample/absorbance of the control) × 100.

2.4 Apoptosis Assay Using Annexin V/PI Staining

Annexin V is a phospholipid-binding protein with high affinity and binds to cell membranes in early apoptosis. Therefore, Annexin V is known as a sensitive index for detecting early cell apoptosis. Propidium iodide (PI) is a nucleic acid dye that cannot pass through an intact cell membrane, but can cross the membrane of apoptotic and

dead cells during middle-late apoptosis due to an increase in permeability. This allows PI to stain the nucleus red. Thus, the combination of Annexin V with PI can be used to distinguish the different periods of cell apoptosis. Adherent cells were digested with 0.25 % trypsin without Ethylene Diamine Tetraacetie Acid (EDTA). The cell suspension was centrifuged at 1500 rpm for 5 to 10 min at room temperature. The cells were washed 3 times with 1 × PBS, and 300 μL of 1 × binding buffer was used to resuspend the astrocytes. Then, the cell suspension was added to 5 μL of Annexin V-FITC and PI, and incubated at room temperature for 15 min. An Annexin V-FITC Apoptosis Detection kit (KeyGen BioTECH, Nanjing, China) was used. Flow cytometric analysis was performed using a BD FACSCalibur flow cytometer (NK, USA) with Cell Quest Pro software.

2.5 Western Blot

After treatment, astrocytes were detached with trypsin/EDTA and collected into tubes. The collected astrocytes were lysed in RIPA lysis buffer (Beyotime Biotechnology, Shanghai, China) containing 1 % protease inhibitors (Beyotime Biotechnology, Shanghai, China). The collected protein samples were centrifuged at 12000 rpm for 10 min. Protein concentrations were determined using an enhanced BCA Protein Assay kit (Beyotime Biotechnology, Shanghai, China), and then denatured with 1 × loading buffer in boiling water for 10 min. Proteins (20 μg) were separated by sodium dodecyl sulfate-polyacrylamide gel electrophoresis (SDS–PAGE) and transferred to PVDF membranes (Amersham). Next, 5 % skim milk in TBST (1 mol/l Tris-HCl (pH 7.5), 0.8 % NaCl, and 0.1 % Tween 20) was used to block the membranes for 1 hour at room temperature. Then, the membranes were incubated with anti-PPARα (Proteintech, Chicago, USA 1:4,000), anti-PPARβ/δ (Proteintech, Chicago, USA 1:7,000), anti-PPARγ (Proteintech, Chicago, USA 1:7,000), anti-GRP78 (Abcam, Chicago, USA 1:1,000), anti-Caspase3 (Abcam, Chicago, USA 1:400), anti-Caspase12 (Abcam, Chicago, USA 1:1,200), anti-CHOP (Cell Signaling, Madrid, Spain 1:1,000), and anti-GAPDH (Proteintech, Chicago, USA 1:5,000) antibodies at 4 °C overnight. The primary antibody was removed and membranes washed 3 times

with TBST for 15 min each wash. Horseradish peroxidase-conjugated goat anti-rabbit secondary antibodies (Proteintech, Chicago, USA 1:10,000) were incubated for 1 hour at room temperature. After the secondary antibody was removed, membranes were washed 3 times with TBST for 15 min each wash. Relative proteins levels were detected using enhanced chemiluminescence reagent and analyzed by ImageJ software.

2.6 RNA Extracts

Total RNA was extracted from the astrocytes that received different treatments using Trizol reagent (Invitrogen Life technologies, California, USA), according to the manufacturer's protocol. The concentration and purity of the total RNA were measured using a NanoDrop 2000 spectrophotometer (NanoDrop Technologies, Thermo Scientific, USA). A reverse transcriptase kit was used to synthesize the complementary DNA, and additional total RNA samples were stored at −80 °C.

2.7 Reverse Transcriptase and Real-time Quantitative PCR

Total RNA (1 μg) was reverse transcribed to synthesize the complementary DNA using a RevertAid First Strand cDNA Synthesis Kit (Thermo Scientific, USA). In accordance with the manufacturer's instructions, the reverse transcription reaction was performed in the thermal cycler (Eppendorf, Germany) with incubation at 65 °C for 5 min, followed by 42 °C for 60 min, and activation at 70 °C for 5 min.

Quantitative real-time PCR was performed using FastStart Universal SYBR Green Master (ROX, Roche Diagnostics, Germany) to determine the mRNA level using an ABI 7300 Real-Time PCR System (Applied Biosystems, USA). The reactions had 20 μL of reactants containing 1 × SYBR Green Master Mix, forward and reverse primers (sequences listed in Table S1) at 10 μM concentration, and a single cDNA sample. Reactions were conducted for 10 min for incubation at 95 °C, followed by 40 cycles at 95 °C for 15 s and 58 °C to 60 °C for 1 min. Amplification specificity was validated by the presence of a single peak in melting curves. GAPDH was used as an endogenous control, and the relative expression of the target gene was determined

using the $2^{(-\Delta\Delta ct)}$ method. To confirm results, each sample was run in triplicate, and experiments were repeated at least 3 times.

Table S1. Primer sequences of target genes for qPCR.

Target Gene	Orientation	Primer Sequence (5'–3')
GAPDH	Forward	GTTTGTGATGGGTGTGAACC
	Reverse	TCTTCTGAGTGGCAGTGATG
PPARα	Forward	ACTGAAAGCAGAAATTCTTACCTGTG
	Reverse	AAGCGTCTTCTCGGCCATA
PPARβ	Forward	CTCCTGCTGACTGACAGATG
	Reverse	TCTCCTCCTGTGGCTGTTC
PPARγ	Forward	CCCACCAACTTCGGAATCAG
	Reverse	GGAATGGGAGTGGTCATCCA

2.8 Reverse Transcriptase and MiRNA Real-time Quantitative PCR

Except for the reverse transcription primer of the TaqMan® MicroRNA assay (Applied Biosystems, Carlsbad, USA), the TaqMan® MicroRNA Reverse Transcription Kit (Applied Biosystems, Carlsbad, USA) was used to synthesize cDNA. In accordance with the manufacturer's instructions, 500 ng of total RNA was incubated at 16 °C for 30 min, followed by incubation at 42 °C for 30 min and reverse transcriptase inactivation at 85 °C for 5 min. This procedure was performed in the thermal cycler (Eppendorf, Germany).

The ABI 7300 Real-Time PCR System (Applied Biosystems, Carlsbad, USA) with TaqMan® Universal Master Mix II (Applied Biosystems, Carlsbad, USA) was used for the miRNA amplification analysis. The U6 and microRNA-181a (miR-181a) primers were purchased as part of the TaqMan® MicroRNA assay (Applied Biosystems, Carlsbad, USA). The reaction system contained 2 × TaqMan® Universal Master Mix □, TaqMan® assay primer and cDNA sample, and the protocol was performed at 95 °C for 10 min, followed by 40 cycles of 15 sec at 95 °C and for 1 min at 60°C. U6 was used as an endogenous control, and the relative expression of

miR-181a was determined using the $2^{(-\Delta\Delta ct)}$ method. To confirm results, each sample was run in triplicate, and experiments were repeated at least 3 times.

2.9 Luciferase Reporter Assay

The wild-type (WT) and mutant versions of the miR-181a response element in the 3'-UTR of HSPA5 were each cloned into miR-report plasmids downstream of the luciferase reporter gene. Plasmids that had been combined with rno-miR-181a and negative control (NC) mimics, along with luciferase reporter constructs containing WT or Mut HSPA5 3'-UTR, were cotransfected into 293T cells. Forty-eight hours after cell transfection, we used the Dual-Luciferase assay system (Promega, USA) to measure luciferase activity. The firefly luciferase value validated the candidate target inhibition gene translation level of miR-181a.

2.10 Nuclear Protein Extracts

Nuclear protein was harvested using an EpiQuik^{TM} Nuclear Extraction Kit (Epigentek, USA). In the case of nuclear extract isolation, 2 to 5 × 10^6 cells were seeded on a 100 mm plate. The treated astrocytes were removed from the growth medium and washed twice with PBS. Astrocytes were detached with trypsin/EDTA and collected in a tube. The cell suspension was centrifuged at 1000 rpm for 5 min, and the supernatant was discarded. The nuclear pellet was incubated with NE1 and then diluted with distilled water at a 1:10 dilution. DTT and PIC were added to ice-cold NE1 diluted at a 1:1000 dilution. Astrocyte pellets were resuspended in 100 μL of diluted NE1 per 10^6 cells. During this 10 min incubation, samples were vortex-mixed 10 times every 3 min. Nuclear extracts were obtained by centrifugation at 12000 rpm for 1 min at 4 °C. Then, the cytoplasmic extract was carefully removed from the nuclear pellet. Based on the pellet size, the nuclear pellets were successively incubated with NE2 containing DTT and PIC at 1:1000 dilutions. The extract was incubated on ice for 15 min and vortexed 5 times every 3 min. Nuclear extracts were obtained by centrifugation at 14000 rpm for 10 min at 4 °C. The protein concentration

was measured using an enhanced BCA Protein Assay kit (Beyotime Biotechnology, Shanghai, China) according to the manufacturer's instruction.

2.11 DNA Methyltransferase **(DNMT) Activity**

Nuclear protein was isolated using the EpiQuik™ Nuclear Extraction Kit (Epigentek, USA), and the nuclear protein was quantified using an enhanced BCA Protein Assay kit (Beyotime Biotechnology, Shanghai, China), as previously described. Ten μg of nuclear protein was used to measure DNMT activity with an EpiQuik™ DNA Methyltransferase Activity/Inhibition Assay Kit (Epigentek, USA), according to the manufacturer's protocol. The optical density was measured on a microplate reader at 450 nm, and the DNMT activity was calculated according to the following formula:

DNMT activity (OD/μg/h) = [(average sample OD - average blank OD) / (protein amount* × hour**)] × 1000

* Protein amount (μg) added to the reaction.

** Incubation time used for the reaction.

2.12 DNMT Expression Determined Using a DNMT Assay Kit

Nuclear protein was isolated using the EpiQuik™ Nuclear Extraction Kit I (Epigentek, USA), and the nuclear protein was quantified using an enhanced BCA Protein Assay Kit (Beyotime Biotechnology, Shanghai, China), as previously described. Seven μg of nuclear protein was used to measure the DNMT activity using an EpiQuik™ DNMT Assay Kit (Epigentek, USA) according to the manufacturer's protocol. A standard curve and the OD value were measured on a microplate reader at 450 nm with an optional reference wavelength of 655 nm. The DNMT expression was calculated according to the following formula:

DNMT expression (OD/μg) = [(average sample OD - average blank OD) / (protein amount* × slope)] × 1000

* Protein amount (μg) added to the reaction.

2.13 DNA Methylation Assay

Genomic DNA (gDNA) was extracted from astrocytes using a DNeasy Blood and Tissue Kit (Tiangen, Beijing, China) according to the manufacturer's protocol. Then, the gDNA was detected using 1.0 % agarose gel electrophoresis. A NAS-99 (ACTGene, USA) was used to measure the gDNA concentrations of our samples. Five hundred micrograms of gDNA was extracted and then bisulfate converted using an EZ DNA Methylation Gold Kit (Zymo Research, Freiburg, Germany). Bisulfite treatment of gDNA converted unmethylated cytosines to uracil, and the respective changes were detected by PCR amplification followed by DNA sequencing. The fragment of interest was amplified from converted DNA by real-time qPCR using Platinum® Taq DNA Polymerase High Fidelity (Thermo Scientific, USA). Isolated plasmid DNA was sequenced, and SnapGene software was used to compare the obtained sequence to the unconverted gDNA.

Table S2. Primer sequences of PCR targets.

Target Gene	Orientation	Primer Sequence (5'-3')	Amplicon Length (bp)
miR-181a$_1$	Forward	GATATAGTAAGAAGTGGAGGTTTGT	430 bp
	Reverse	ATTCAATAAACTTTTCTACACAATTC	
miR-181a$_2$	Forward	TTGATAGATTTTTGTAGTAGAAATTG	353 bp
	Reverse	CACTCATAACTCAAAATTAAACCTT	

2.14 Statistical Analysis

The data obtained are presented as the mean ± SEM of at least 3 independent experiments. The relationship between 2 factors was analyzed using Pearson correlation analysis, and bootstrapping was used in paired samples tests. Groups were compared using a 2-way ANOVA with post hoc Bonferroni's multiple comparisons test and using 1-way ANOVA with post hoc Tukey's multiple comparisons test. All analyses used GraphPad Prism 6.0 software. A value of $P < 0.05$ indicated that the difference was statistically significant.

3. Results

3.1 PPARβ/δ Dominantly Expressed Subtype in the Primary Cultured Astrocytes

The 3 known PPAR isoforms, PPARα, PPARβ/δ, and PPARγ, have different tissue distributions and functional activity. In the present study, we found that the 3 subtypes of PPARs were expressed in the primary cultured astrocytes, and the PPARβ/δ subtype had the highest expression of all PPAR subtypes. This was determined using real-time PCR (Fig. 1a). To confirm the above results, we also measured the protein expression of the 3 subtype PPARs by immunoblot; these subtypes corresponded to MWs of 52 kDa, 50 kDa, and 58 kDa, respectively (Fig. 1b). Results show that the basal level of PPARα, PPARβ/δ, and PPARγ was 21.22 %, 53.49 %, and 34.11 %, respectively (Fig. 1b). Western blot analysis also revealed that PPARβ/δ was the dominant subtype in astrocytes.

3.2 PPARβ/δ Activation Protects Against Corticosterone-induced Astrocyte Damage

Corticosterone treatment induces astrocyte impairment. As shown in Fig. 2a, the viability of astrocytes significantly decreased by 14 %, 24 %, and 24 % compared with the control groups, respectively, following treatments with corticosterone at 1, 10, and 100 μM concentrations for 24 hours. Results indicated that corticosterone induced astrocytic injury in a concentration-dependent manner. We thus chose 10 μM corticosterone for subsequent studies.

As shown Fig. 2b, astrocyte viability was restored to 95.32 % by treatment with the PPARβ/δ agonist GW0742 at a concentration of 10 μM. The protective effects of GW0742 were prevented by the PPARβ/δ antagonist GSK3787 (Fig. 2c), suggesting that PPARβ/δ activation exerted significant neuroprotective effects against corticosterone-induced astrocyte damage. In addition, GSK3787 alone had no toxic effect on astrocytes (Fig. 2d).

Simultaneously, we found that corticosterone treatment reduced the mRNA and protein expression levels of PPARβ/δ, and this effect could be attenuated by GW0742 (Fig. 2e and 2f).

3.3 PPARβ/δ Activation Attenuates Corticosterone-induced Endoplasmic Reticulum (ER) Stress in Astrocytes

Glucose regulated protein 78 (GRP78) and CCAAT/enhancer-binding protein homologous protein (CHOP), which reflect the status of ER stress, were monitored in our studies. As shown in Fig. 3, Western blot analyses demonstrated that corticosterone significantly increased the expression of GRP78 (MW 75kDa) and CHOP (MW 27kDa). Meanwhile, the PPARβ/δ agonist GW0742 completely prevented the corticosterone-induced increase in GRP78 and CHOP levels. Furthermore, the inhibitory effect of PPARβ/δ activation was blocked by the PPARβ/δ antagonist GSK3787. Therefore, our results suggest that inhibition of corticosterone-induced ER stress is responsible for the protective effect of PPARβ/δ activation.

3.4 PPARβ/δ Activation Protects Against ER Stress-induced Astrocyte Apoptosis

To further examine whether the ER stress-mediated apoptosis was involved in astrocyte degeneration and the effects of PPARβ/δ activation on ER-specific apoptosis, we measured astrocyte apoptosis using an Annexin V-FITC/PI double-staining assay and then determined the ER-specific expression of apoptosis markers using Western blot. The percentage of apoptotic astrocytes (including early and late apoptosis cells) remarkably increased following corticosterone treatment (Fig. 4a). This corticosterone-induced astrocyte apoptosis was reduced by GW0742, and only 6 % of GW0742-treated astrocytes were apoptotic (Fig. 4a). GSK3787 blocked the anti-apoptosis effects of GW0742.

Prolonged ER stress leads to apoptosis via activation of the cascade of caspase-12 and caspase-3 (Tong et al., 2015). Our results showed that corticosterone caused significant increases in caspase-12 expression in astrocytes, which was prevented by

GW0742 (Fig. 4b). As shown in Fig. 4c, the control astrocytes constitutively expressed moderate quantities of pro-caspase-3 protein and rather low levels of cleaved caspase-3. Furthermore, although corticosterone significantly increased the ratio of cleaved caspase-3 to pro-caspase-3 in astrocytes, GW0742 treatment could reverse this increase. Our data confirm the idea that activating PPARβ/δ relieves ER stress-mediated astrocyte apoptosis.

3.5 PPARβ/δ Activation Up-regulates MiR-181a Levels in Astrocytes

Previous reports suggested that miR-181a targeted GRP78 (Ouyang et al., 2012). In our study, a dual-luciferase reporter gene assay was used to confirm that GRP78 was a direct target of miR-181a. We found that transfection with miR-181a resulted in an approximately 30 % reduction in HSPA5-3'UTR gene luciferase activity, but failed to affect mutant HSPA5-3'UTR gene luciferase. Our results confirm that miR-181a directly binds to the 3'UTR of GRP78 and inhibits GRP78 expression (Fig. 5b).

Then, we tested the effects of PPARβ/δ activation on endogenous miR-181a expression in astrocytes. As expected, the expression level of miR-181a was remarkably reduced in corticosterone-treated astrocytes. Treatment with GW0742 abolished the down-regulation of miR-181a induced by corticosterone (Fig. 5c). These results suggest that activating PPARβ/δ increases miR-181a and thereby inhibits corticosterone-induced ER stress.

3.6 PPARβ/δ Activation Inhibits the Activity and Expression of DNMTs and Prevents the CpG Island Methylation of MiR-181a1 in Astrocytes

Since DNA methylation might contribute to the down-regulation of miRNAs in major cells, we evaluated the effects of GW0742 on DNMT activities in astrocytes (Fig. 6a). Results showed that corticosterone could augment DNMT activities, and this effect could be reversed by GW0742. Additionally, GSK3787 antagonized the inhibitory effects of GW0742 on DNMT activities.

Furthermore, we examined the effects of GW0742 on the expression of DNMT1, DNMT3a, and DNMT3b in astrocytes (Fig. 6b). Their expression levels were

dramatically up-regulated by corticosterone, and increases were inhibited by GW0742. GSK3787 also antagonized this effect of GW0742 (Fig. 6b). Conclusively, our data revealed that activating PPARβ/δ inhibits DNA methyltransferase activity and expression, which may contribute to decreased miR-181a levels.

CpG island hypermethylation is associated with the transcriptional silencing of genes that encode miRNAs. To validate the inhibitory effects of PPARβ/δ activation on DNA methylation, we determined the methylation status of the targeted CpG sites of miR-181a in 4 groups via bisulfite sequencing analysis. The CpG island was predicted to occur in the murine miR-181a promoter region (Fig. 6c). The result was consistent with DNMT activity and expression results, and the CpG DNA methylation levels of miR-181a1 were highest in the corticosterone-treated astrocytes. Sixty percent of the sites were methylated in the corticosterone-treated astrocytes, and this methylation was limited by GW0742 (Fig. 6d, 6f). Additionally, there was no difference in the methylation levels of miR-181a2 among the 3 groups (Fig. 6e, 6g). These results suggest that the CpG island DNA methylation of miR-181a1 was associated with miR-181a silencing in astrocytes, which is responsible for the up-regulation effects of PPARβ/δ on miR-181a expression.

4. Discussion

Astrocytes take part in a variety of functions in the CNS, including providing structural, metabolic, and trophic support for neurons (Araque et al., 1999; Garcia-Segura et al., 2004). Moreover, although chronic corticosterone stimulation has been shown to induce astrocytic loss in brain disorders, the involved mechanism remains unclear. PPARs are ligand-activated transcription factors implicated in regulating metabolic reactions. Moreover, increasing evidence reveals that PPARs play neuroprotective roles in various neurodegenerative disease models *in vivo* and *in vitro* (Ouk et al., 2014; Carta et al., 2013a; Carta et al., 2013b). First, the present study showed that PPARα, PPARβ/δ, and PPARγ were expressed in the primary cultured

astrocyte, and PPARβ/δ was the dominant subtype. Then, we investigated the roles of PPARβ/δ in corticosterone-induced cellular injury in astrocytes.

Chronic corticosterone treatment induces a depressive behavior accompanied by astrocytic degeneration or dysfunction (Sanacora et al., 2013; Smiałowska et al., 2013; Kong et al., 2014; Rajkowska et al., 2007). The present results concur with literature by showing that treatment for 24 hours with corticosterone causes loss of astrocyte activities (Chatterjee et al., 2013). We also found that corticosterone treatment resulted in decreases in the mRNA and protein expressions of PPARβ/δ. GW0742 up-regulated PPARβ/δ, which protected against corticosterone-induced decline in astrocyte vitality. These effects were blocked by PPARβ/δ antagonist GSK3787. Our results reveal that the neuroprotective action in astrocytes is concerned with PPARβ/δ activation.

ER is a subcellular compartment playing an essential role in folding and processing membrane and secretory proteins, and thus, its well-ordered operation is indispensable for normal cell functioning and survival (Gulyaeva, 2015). However, exposure to devastating stress damages ER homeostasis, leading to an adaptive unfolded protein response (UPR) to compensate damage (Ron et al., 2002; Kadowaki et al., 2004; Marciniak et al., 2006; Xu et al., 2005). Additionally, CHOP and GRP78 are critical mediators in the course of ER stress-mediated apoptosis (Gulyaeva, 2015). We found that chronic corticosterone treatment increased the expressions of GRP78 and CHOP, inducing greater ER stress. PPARβ/δ agonist GW0742 significantly inhibited the expressions of GRP78 and CHOP, suggesting that PPARβ/δ activation protected against corticosterone-induced ER stress. On the other hand, caspase-12 mediates the ER stress-specific apoptotic pathway (Nakagawa et al., 2000), and its activation leads to caspase-3 activation and cellular death (Tong et al., 2015). In our experiments, corticosterone resulted in astrocytic apoptosis, which was well-correlated with the elevated expressions of caspase-12 and cleaved-caspase-3. Treatment with GW0742 remarkably attenuated the corticosterone-induced increase in the levels of caspase-12 and cleaved-caspase-3, and thereby suppressed astrocytic apoptosis. Conclusively,

these results reveal that activation of PPARβ/δ protects against corticosterone-induced ER stress and subsequent ER-specific apoptosis.

As endogenous regulators, miRNAs play important roles in modulating gene expression. It was reported that GRP78 is negatively regulated by miR-181a (Ouyang et al., 2012). Moreover, Hutchison et al. (date) discussed that miR-181 expression is developmentally regulated and enriched in astrocytes compared to neurons. These data support a possible role for miR-181a in cell fate in the CNS and warrant further investigation (Hutchison et al., 2013). Therefore, we determined whether miR-181a was involved in the regulating effects of PPARβ/δ in ER stress. We confirmed that miR-181a directly targeted the 3'UTR of GRP78, which was indicated by suppressed luciferase activity. Moreover, our results showed that corticosterone decreased miR-181a expression in astrocytes. GW0742 treatment reversed this effect. Therefore, activating PPARβ/δ up-regulated miR-181a and then inhibited GRP78 expression.

Finally, we revealed the mechanisms involved in GW0742-induced up-regulation of miR-181a. DNA methylation is an enzyme-mediated modification to DNA that is an important epigenetic mechanism to silence genes transcribed by RNA polymerase II (Cheng et al., 2010). Therefore, it is possible that DNA methylation regulates miRNA expression. There are 3 DNMT subtypes in mammalian cells, DNMT1, DNMT3a and DNMT3b, which generally perform de novo DNA methylation. In our studies, corticosterone exposure in astrocytes not only increased DNMT expression, but also enhanced their activities. Furthermore, PPARβ/δ agonist GW0742 inhibited these expressions and activities. Additionally, DNMTs regulate promoter DNA methylation and maintain the methylation status for silencing gene expression (Goll et al., 2005; Turek-Plewa et al., 2005). Results from bisulfite sequencing analysis and the luciferase activity assay showed that corticosterone treatment resulted in higher CpG methylation, which promoted miR-181a and was inhibited by GW0742. In summary, on the basis of our findings we propose that PPARβ/δ activation prevents ER stress in astrocytes through suppressing DNA methylase and thereby up-regulating miR-181a expression.

5. Conclusions

The present study revealed that PPARβ/δ is the dominant subtype expressed in primary cultured astrocytes, and its activation inhibits corticosterone-induced ER stress and astrocyte apoptosis. Our results also demonstrated that PPARβ/δ activation suppresses CpG island hypermethylation-associated silencing of microRNA-181a, and thereby down-regulates the ER stress-related protein GRP78 in astrocytes (As shown in Figure 7). Our findings suggest that PPARβ/δ activation in astrocytes might be a promising target for regulating ER stress-induced astrocytic injury.

Acknowledgements

This study was supported by grants from the National Natural Science Foundation of China (No.81273495and No.81473197) and Major Project of Jiangsu Provincial Department of Education (No.12KJA310002).

Author contributions

Conceived, designed and wrote the experiments: Xiu-Lan Sun. Performed the experiments: Juan Ji, Xiao-Ning Zeng, Lu-Lu Cao, Ling Zhang. Analyzed data: Juan Ji, Xiao-Ning Zeng. Contributed reagents/materials/analysis tools: Juan Ji, Xiao-Ning Zeng, Zhan Zhao, Dan-Dan Yang, Xiu-Lan Sun.

Reference

Allaman I., Belanger M., Magistretti P.J. Astrocyte-neuron metabolic relationships: for better and for worse. Trends Neurosci. 2011;34:76-87.

Araque A., Parpura V., Sanzgiri R.P., Haydon P.G. Tripartite synapses: Glia, the unacknowledged partner. Trends Neurosci. 1999;22(5):208-215.

Banasr M, Duman RS. Glial loss in the prefrontal cortex is sufficient to induce depressive-like behaviors. Biol Psychiatry. 2008; 64(10): 863-870.

Carta AR. PPARγ: therapeutic prospects in Parkinson's disease. Curr Drug Targets. 2013;14(7):743-751.

Carta AR, APisanu. Modulating microglia activity with PPARγ agonists: a promising therapy for Parkinson's disease. Neurotox Res. 2013;3(2):112-123.

Chatterjee S., Sikdar S.K. Corticosterone treatment results in enhanced release of peptidergic vesicles in astrocytes via cytoskeletal rearrangements. Glia. 2013;61(12):2050-2062.

Cheng X., Blumenthal R.M. Coordinated Chromatin Control: Structural and Functional Linkage of DNA and Histone Methylation. Biochemistry. 2010;49(14):2999-3008.

Czeh B, Lucassen PJ. What causes the hippocampal volume decrease in depression? Are neurogenesis, glial changes and apoptosis implicated? Eur Arch Psychiatry Clin Neurosci. 2007;257:250-260.

Desvergne B., Wahli W. Peroxisome proliferator activated receptors:nuclear control of metabolism. Endocr Rev. 1999;20:649-688.

Garcia-Segura L.M., McCarthy M.M. Minireview: Role of glia in neuroendocrine function. Endocrinology. 2004;145(3):1082-1086.

Goll M.G., Bestor T.H. Eukaryotic cytosine methyltransferases. Annual Review of Biochemistry. 2005;74(1):481-514.

Gulyaeva N.V. Brain ischemia, endoplasmic reticulum stress, and astroglial activation: new insights. Journal of Neurochemistry. 2015;132(3):263-265.

Guo WZ, Miao YL, An LN, Wang XY, Pan NL, Ma YQ, Chen HX, Zhao N, Zhang H, Li YF, Mi WD. Midazolam provides cytoprotective effect during corticosterone-induced damages in rat astrocytes by stimulating steroidogenesis. Neurosci Lett. 2013;547:53-58.

Heneka M.T., Landreth G.E. Ppars in the brain. Biochim Biophys Acta. 2007;1771(8):1031-1045.

Hetz C, Chevet E, Harding HP. Targeting the unfolded protein response in disease.

Nat Rev Drug Discov. 2013;12:703-719.

Hutchison ER, Kawamoto EM, Taub DD, Lal A, Abdelmohsen K, Zhang Y, Wood WH, Lehrmann E, Camandola S, Becker KG, Gorospe M, Mattson MP. Evidence for miR-181 involvement in neuroinflammatory responses of astrocytes. Glia. 2013;61(7):1018-1028.

Joardar A, Menzl J, Podolsky TC, Manzo E, Estes PS, Ashford S, Zarnescu DC. PPAR gamma activation is neuroprotective in a Drosophila model of ALS based on TDP-43. Hum Mol Genet. 2015;24(6):1741-1754.

Kadowaki H., Nishitoh H., Ichijo H. Survival and apoptosis signals in ER stress: the role of protein kinases. Journal of Chemical Neuroanatomy. 2004;28(1-2):93-100.

Kong H, Zeng XN, Fan Y, Yuan ST, Ge S, Xie WP, Wang H, Hu G. Aquaporin-4 Knockout Exacerbates Corticosterone-Induced Depression by Inhibiting Astrocyte Function and Hippocampal Neurogenesis. CNS Neurosci Ther. 2014;20(5):391-402.

Law YW, Yip PS, Zhang Y, Caine ED. The chronic impact of work on suicides and under-utilization of psychiatric and psychosocial services. J Affect Disord. 2014;168: 254-261.

Lussier AL, Lebedeva K, Fenton EY, Guskjolen A, Caruncho HJ, Kalynchuk LE. The progressive development of depression-like behavior in corticosterone-treated rats is paralleled by slowed granule cell maturation and decreased reelin expression in the adult dentate gyrus. Neuropharmacology. 2013;71:174-183.

Mandrekar-Colucci S, Sauerbeck A, Popovich PG, McTigue DM. PPAR agonists as therapeutics for CNS trauma and neurological diseases. ASN Neuro. 2013;5(5):e00129.

Marciniak S.J., Ron D. Endoplasmic Reticulum Stress Signaling in Disease. Physiological Reviews. 2006;86(4):1133-1149.

Martin HL, Mounsey RB, Sathe K, Mustafa S, Nelson MC, Evans RM,Teismann P. A peroxisome proliferator-activated receptor-δ agonist provides neuroprotection in the 1-methyl-4-phenyl-1,2,3,6-tetrahydropyridine model of Parkinson's disease. Neuroscience. 2013;240:191-203.

Moreno S., Farioli-Vecchiol S., Cerù M.P. Immunolocalization of peroxisome proliferator-activated receptors and retinoid X receptors in the adult rat Cns. Neuroscience. 2004;123(1):131-145.

Nakagawa T., Zhu H., Morishima N., Li E., Xu J.,Yankner B.A. Caspase-12 mediates endoplasmic-reticulum-specific apoptosis and cytotoxicity by amyloid-beta. Nature. 2000;403(6765):98-103.

Obara M., Szeliga M., Albrecht J. Regulation of pH in the mammalian central nervous system under normal and pathological conditions: facts and hypotheses. Neurochem Int. 2008;52(6):905-919.

Ouk T, Potey C, Laprais M, Gautier S, Hanf R, Darteil R, Staels B, Duriez P, Bordet R. PPARα is involved in the multitargeted effects of a pretreatment with atorvastatin in experimental stroke. Fundam Clin Pharmacol. 2014;28(3): 294-302.

Ouyang YB, Lu Y, Yue S, Xu LJ, Xiong XX, White RE, Sun X, Giffard RG. miR-181 regulates GRP78 and influences outcome from cerebral ischemia in vitro and in vivo. Neurobiol Dis. 2012; 45(1):555-63.

Papadopoulos M.C., Verkman A.S. Aquaporin water channels in the nervous system. Nat Rev Neurosci. 2013;14(4):265-277.

Patti Waters, Cheryl M., McCormick. BCaveats of chronic exogenous corticosterone treatments in adolescent rats and effects on anxiety-like and depressive behavior and hypothalamic-pituitary-adrenal (HPA) axis function. Biol Mood Anxiety Disord 2011;1(1):4.

Pellerin L. Brain energetics (thought needs food). Curr Opin Clin Nutr Metab Care. 2008;11(6):701-705.

Rajkowska G, Stockmeier CA.Astrocyte pathology in major depressive disorder: insights from human postmortem brain tissue.Curr Drug Targets. 2013;14(11):1225-1236.

Rajkowska G., Miguel-Hidalgo J.J. Gliogenesis and Glial Pathology in Depression. CNS Neurol Disord Drug Targets. 2007;6(3):219-233.

Rash J.E. Molecular disruptions of the panglial syncytium block potassium siphoning and axonal saltatory conduction:pertinence to neuromyelitis optica and other demyelinating diseases of the central nervous system. Neuroscience. 2010;168(4):982-1008.

Ron D. Translational control in the endoplasmic reticulum stress response.J Clin Invest.2002;110:1383–1388.

Sanacora G., Banasr M.From pathophysiology to novel antidepressant drugs: glial contributions to the pathology and treatment of mood disorders. Biol Psychiatry. 2013;73(12):1172-1179.

Sattler R., Rothstein J.D. Regulation and dysregulation of glutamate transporters. Handb Exp Pharmacol. 2006;175:277-303.

Schousboe A., Sarup A., Bak L.K., Waagepetersen H.S., Larsson O.M. Role of astrocytic transport processes in glutamatergic and GABAergic neurotransmission. Neurochem Int. 2004;45:521-527.

Shaha A, Kumar A. Methamphetamine-mediated endoplasmic reticulum (ER) stress induces type-1 programmed cell death in astrocytes via ATF6, IRE1α and PERK pathways. Oncotarget. 2016.

Sibille J., Pannasch U., Rouach N. Astroglial potassium clearance contributes to short-term plasticity of synaptically evoked currents at the tripartite synapse. J. Physiol. 2014;592:87-102.

Simard M., Nedergaard M. The neurobiology of glia in the context of water and ion homeostasis. Neuroscience. 2004;129(4):877-896.

Smiałowska M., Szewczyk B., Woźniak M., Wawrzak-Wleciał A., Domin H. Glial degeneration as a model of depression. Pharmacol Rep. 2013;65(6):1572-1579.

Strokin M., Sergeeva M., Reiser G. Role of Ca2+-independent phospholipase A2 and n-3 polyunsaturated fatty acid docosahexaenoic acid in prostanoid production in brain:

perspectives for protection in neuroinflammation. Int J Dev Neurosci. 2004;22(7):551-557.

Takuma K, Baba A, Matsuda T. Astrocyte apoptosis: implications for neuroprotection. Prog Neurobio. 2004;72:111-127.

Turek-Plewa J., Jagodziński P. The role of mammalian DNA methyltransferases in the regulation of gene expression. Cell Mol Biol Lett. 2005;10:631-647.

Tong Q., Wu L., Gao Q., Ou Z., Zhu D., Zhang Y. PPARβ/δ Agonist Provides Neuroprotection by Suppression of IRE1α Caspase-12 Mediated Endoplasmic Reticulum Stress Pathway in the Rotenone Rat Model of Parkinson's Disease. Mol Neurobiol. 2015.

Vittoria Simonini M, Polak PE, Boullerne AI, Peters JM, Richardson JC, Feinstein DL. Regulation of oligodendrocyte progenitor cell maturation by PPARδ: effects on bone morphogenetic proteins. ASN Neuro. 2010;2(1):e00025.

Wahli W., Michalik L. PPARs at the crossroads of lipid signaling and inflammation. Trends Endocrinol Metab. 2012;23:351-63.

Wilhelm F., Hirrlinger J. Multifunctional roles of NAD+ and NADH in astrocytes. Neurochem. Res. 2012;37:2317-2325.

Xia M, Abazyan S, Jouroukhin Y, Pletnikov M. Behavioral sequelae of astrocyte dysfunction: focus on animal models of schizophrenia. Schizophr Res. 2014.

Xu C., Bailly-Maitre B., Reed J.C. Endoplasmic reticulum stress: cell life and death decisions. Journal of Clinical Investigation. 2005;115(10):2656-2664.

Zhou AX, Tabas I. The UPR in atherosclerosis. Semin Immunopathol. 2013;35:321-332.

Figure legends

Figure 1. PPARβ/δ is the dominant subtype expressed in primary cultured astrocytes. (a) The mRNA expression levels of 3 types of PPARs measured in normal astrocytes (n = 4; $F = 52.55 > F_{0.01\ (1,\ 6)}$; $^{**}P < 0.01$ PPARα group vs. PPARβ/δ group; $^{\#\#}P < 0.01$ PPARβ/δ group vs. PPARγ group); (b) The protein expression levels of 3 types of PPARs measured in normal astrocyte protein (n = 4; $F = 13.92 > F_{0.01\ (1,\ 6)}$;

$^{**}P < 0.01$ PPARα group vs. PPARβ/δ; $^{\#}P < 0.05$ PPARβ/δ group vs. PPARγ group). The total PPARs was used as an internal reference. Groups were compared using 1-way ANOVA with post hoc Tukey's multiple comparisons test.
All data are presented as the mean ± SEM.

Figure 2. PPARβ/δ activation protects against corticosterone-induced astrocyte damage. (a) Astrocytes treated with Cort at concentrations of 1, 10, and 100 μM(n = 4; $F = 329.412 > F_{0.01\,(3,\,12)}$; $^{**}P < 0.01$ vs. Con group); (b) MTT assay performed 24 hours after treatment with Cort (10 μM) and GW (0.1, 1, and 10 μM) (n = 5; $F = 7.402 > F_{0.01\,(4,\,20)}$; $^{**}P < 0.01$ vs. Con group; $^{\#}P < 0.05$ vs. Cort. group); (c) MTT assay performed after 24 hours of treatment with Cort (10 μM), GW (10 μM), and GSK (10 μM) (n = 4; $F = 42.431 > F_{0.01\,(3,\,12)}$; $^{**}P < 0.01$ vs. Con group; $^{\#\#}P < 0.01$ vs. Cort group; $^{\dagger\dagger}P < 0.01$ vs. GW group); (d) MTT assay performed 24 hours after treatment with GSK (0.1, 1, and 10 μM) (n = 4; $F = 1.659 < F_{0.01\,(3,\,12)}$; $P > 0.05$ vs. Con group); (e) PPARβ/δ expression levels measured by RT-qPCR (n = 4; $F = 27.018 > F_{0.01\,(3,\,12)}$; $^{**}P < 0.01$ vs. Con group; $^{\#}P < 0.05$ vs. Cort group; $^{\dagger}P < 0.05$ vs. GW group); (f) PPARβ/δ expression levels measured by Western blot (n = 4; $F = 34.723 > F_{0.01\,(3,\,12)}$; $^{**}P < 0.01$vs. Con group; $^{\#\#}P < 0.01$ vs. Cort group; $^{\dagger}P < 0.05$ vs. GW group). Groups were compared using 1-way ANOVA with post hoc Tukey's multiple comparisons test. Each data point represents the mean ± SEM. Con, Control; Cort, Corticosterone; GW, GW0742; GSK, GSK3787.

Figure 3. PPARβ/δ activation attenuates corticosterone-induced endoplasmic reticulum stress in astrocytes. (a) Western blot analysis of the expression of GRP78 (b) and CHOP (c) in different treatment groups. GRP78 levels were quantified and normalized to the GAPDH levels (n = 5; $F = 8.768 > F_{0.01\,(3,\,16)}$; $^{**}P < 0.01$ vs. Con group; $^{\#\#}P < 0.01$ vs. Cort group; $^{\dagger}P < 0.05$ vs. GW group). CHOP levels were quantified and normalized to the GAPDH levels (n = 4; $F = 23.216 > F_{0.01\,(3,\,12)}$; $^{**}P < 0.01$ vs. Con group; $^{\#\#}P < 0.01$ vs. Cort group; $^{\dagger}P < 0.05$ vs. GW group). Groups were compared using 1-way ANOVA with post hoc Tukey's multiple comparisons test. The data are presented as the mean ± SEM. Con, Control; Cort, Corticosterone; GW, GW0742; GSK, GSK3787.

Figure 4. PPARβ/δ activation protects against ER stress-induced apoptosis of astrocytes. (a) Apoptosis levels of astrocytes determined via flow cytometry (n = 4; $F = 19.795 > F_{0.01\,(3,\,12)}$; $^{**}P < 0.01$ vs. Con group; $^{\#\#}P < 0.01$ vs. Cort group; $^{\dagger\dagger}P < 0.01$ vs. GW group); (b) Western blotting used to analyze the expression of caspase-12. The caspase-12 levels were quantified and normalized to the GAPDH levels (n = 6; $F = 23.785 > F_{0.01\,(3,\,20)}$; $^{**}P < 0.01$ vs. Con group; $^{\#\#}P < 0.01$ vs. Cort group; $^{\dagger\dagger}P < 0.01$ vs. GW group); (c) Western blotting used to analyze the ratio of cleaved caspase-3 to caspase-3 of the different groups (n = 4; $F = 10.419 > F_{0.01\,(3,\,12)}$; $^{**}P < 0.01$ vs. Con group; $^{\#}P < 0.05$ vs. Cort group; $^{\dagger}P < 0.05$ vs. GW group). Groups were compared using 1-way ANOVA with post hoc Tukey's multiple comparisons test. The data are

presented as the mean ± SEM. Con, Control; Cort, Corticosterone; GW, GW0742; GSK, GSK3787.

Figure 5. PPARβ/δ activation up-regulates miR-181a in astrocytes. (a) Renilla/firefly luciferase sequences under regulation of HSPA5 3' UTRs were used for transient reporter assay experiments. The wild-type (WT) and mutant (mut) alleles for the miR-181a binding sites are presented. The miR-181a "seed" region and the complimentary 3' UTR sequence are marked in bold. Mutagenic nucleotides are in red and bolded (n = 4; $F = 9.064 > F_{0.01\ (3,\ 12)}$; $^{**}P < 0.01$ vs. Con group; $^{\#}P < 0.05$ vs. Cort group; $^{\dagger}P < 0.05$ vs. GW group); (b) Luciferase activity 48 hours after the co-transfection of miR-181a combined with Renilla/firefly luciferase constructs under regulation of the CDKN1A/TASK1 3' UTR. The data presented are the relative expression level of firefly luciferase standardized to Renilla luciferase (n = 4; $F = 145.6 > F_{0.01\ (1,\ 6)}$; $^{*}P < 0.05$ vs. mimics NC group); (c) MiR-181a expression measured using RT-qPCR (n = 4; $F = 9.064 > F_{0.01\ (3,\ 12)}$; $^{**}P < 0.01$ vs. Con group; $^{\#}P < 0.05$ vs. Cort group; $^{\dagger}P < 0.05$ vs. GW group). Groups were compared using a 2-way ANOVA with post hoc Bonferroni's multiple comparisons test and 1-way ANOVA with post hoc Tukey's multiple comparisons test. The data are presented as the mean ± SEM. Con, Control; Cort, Corticosterone; GW, GW0742; GSK, GSK3787.

Figure 6. PPARβ/δ activation inhibits the activities and expression of DNA methyltransferases (DNMTs) and prevents the CpG island methylation of miR-181a1 in astrocytes. (a) DNMT activities of astrocytes measured using a methyltransferase activity assay kit (n = 5; $F = 11.61 > F_{0.01\ (3,\ 16)}$; $^{*}P < 0.05$ vs. Con group; $^{\#}P < 0.05$ vs. Cort group; $^{\dagger}P < 0.01$ vs. GW group); (b) Expression levels of DNMT1, DNMT3a, and DNMT3b measured using assay kits (n = 4; $F = 298.1 > F_{0.01\ (3,\ 12)}$; $^{**}P < 0.01$, $^{*}P < 0.05$ vs. Con group; $^{\#\#}P < 0.01$, $^{\#}P < 0.05$ vs. Cort group; $^{\dagger\dagger}P < 0.01$, $^{\dagger}P < 0.05$ vs. GW group); (c) CpG island (blue) predictions in the rat miR-181a gene promoter. Suitable primers were designed to amplify the CpG region. PPARβ/δ activation inhibits DNA methylation in the rat miR-181a gene promoter. Methylation levels of (d) miR-181a1 and (e) miR-181a2 in astrocytes. Each row and circle indicates 1 single sequencing reaction and 1 CpG site, respectively. The empty and solid circles refer to the un-methyl and methyl CpG sites, respectively. (f) Quantitative results for miR-181a1 methylation levels (n = 4; $F = 15.18 > F_{0.01\ (3,\ 8)}$; $^{**}P < 0.01$ vs. Con group; $^{\#}P < 0.05$ vs. Cort group). (g) Quantitative results for miR-181a2 methylation levels (n = 4; $F = 1.429 < F_{0.01\ (3,\ 8)}$). Groups were compared using a 2-way ANOVA with post hoc Bonferroni's multiple comparisons test and 1-way ANOVA with post hoc Tukey's multiple comparisons test. The data are presented as the mean ± SEM of 4 independent experiments. Con, Control; Cort, Corticosterone; GW, GW0742; GSK, GSK3787.

Figure 7. PPARβ/δ is the dominant subtype expressed in the primary cultured astrocytes. PPARβ/δ activation inhibits corticosterone-induced ER stress and

astrocytic apoptosis. The protective mechanisms of PPARβ/δ activation include suppressing CpG island hypermethylation-associated silencing of microRNA-181a, and thereby down-regulating ER stress-related protein GRP78 in astrocytes. Our findings suggest that activation of PPARβ/δ in astrocytes might be a promising target for regulating ER stress in depression.

Figure 1

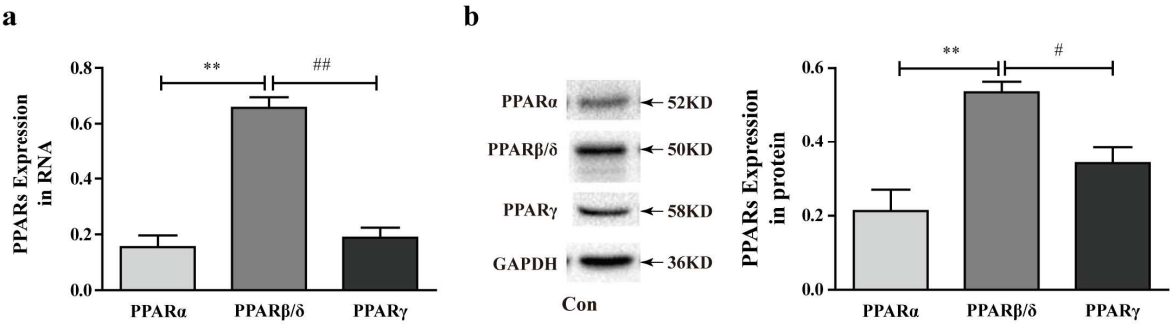

Figure 2

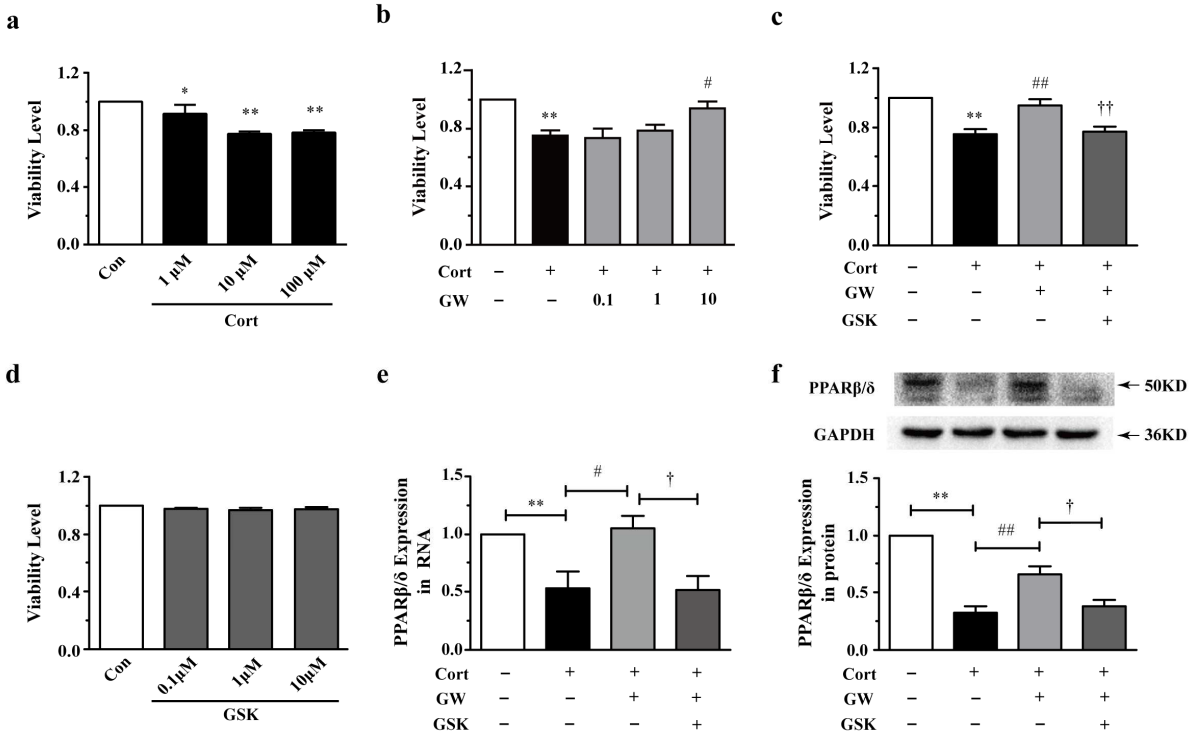

Figure 3

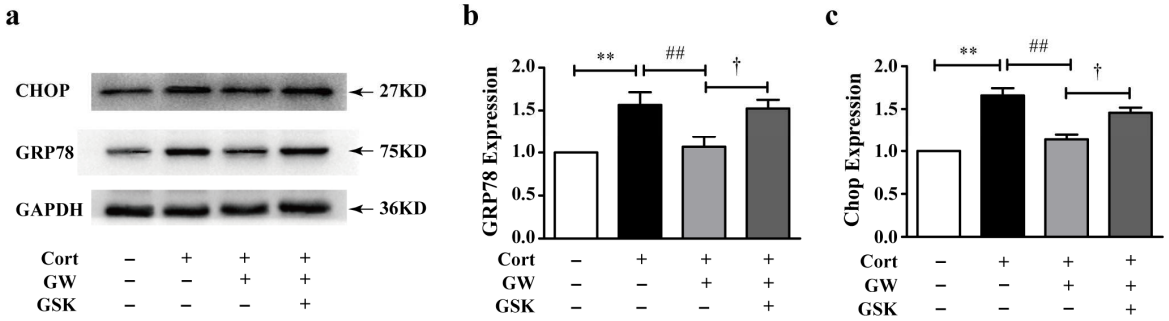

Figure 4

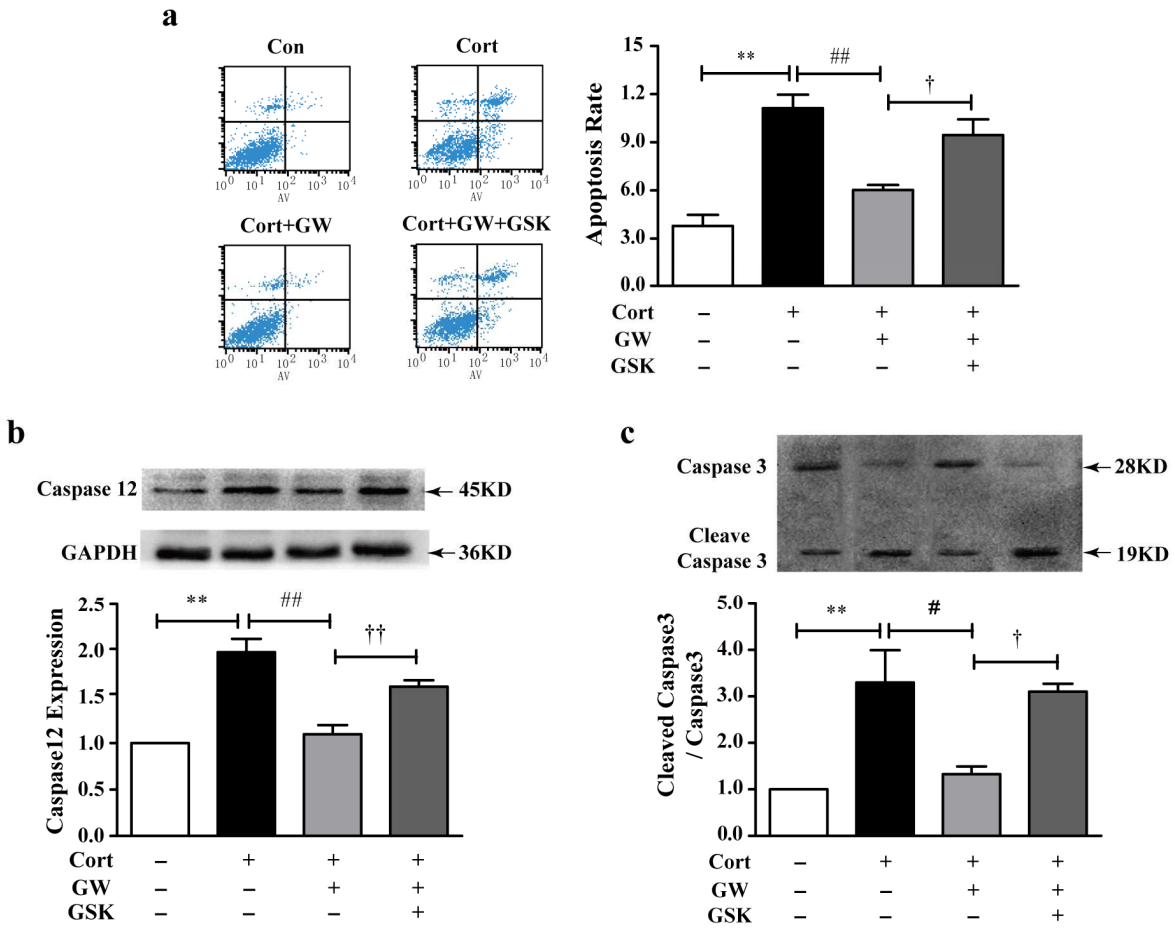

Figure 5

a

```
3'  UGAGUGGCUGUCGCAACUUACAA      rno-miR-181a
                  ||||||
5'  ...GAGAACUUAAGUCUCGAAUGUAA...  HSPA5 WT
5'  ...GAGAACUUAAGUCUCCUUACAAA...  HSPA5 Mut
```

b

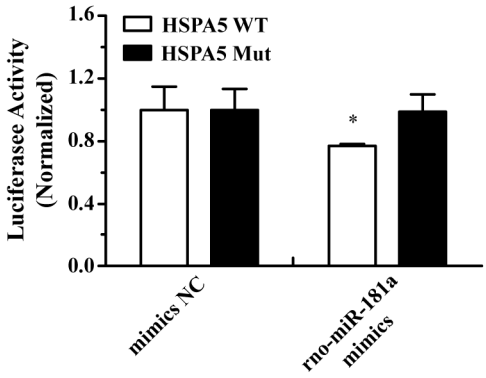

c

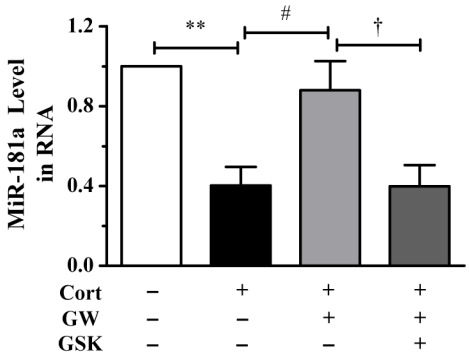

Figure 6

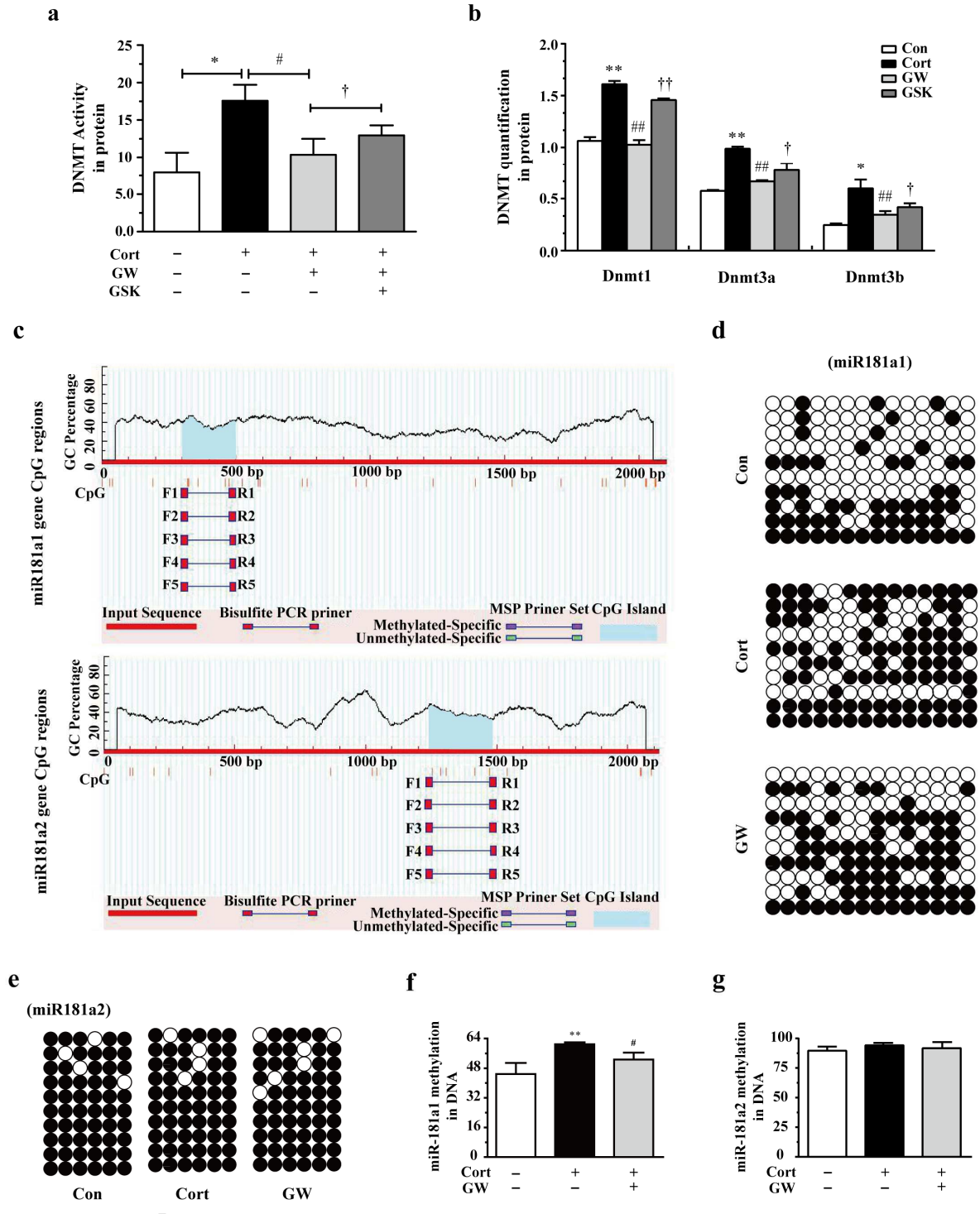
a
DNMT Activity in protein
Cort
GW
GSK
b
DNMT quantification in protein
Con
Cort
GW
GSK
Dnmt1
Dnmt3a
Dnmt3b
c
miR181a1 gene CpG regions
GC Percentage
CpG
Input Sequence
Bisulfite PCR priner
MSP Priner Set
CpG Island
Methylated-Specific
Unmethylated-Specific
miR181a2 gene CpG regions
d
(miR181a1)
Con
Cort
GW
e
(miR181a2)
Con
Cort
GW
f
miR-181a1 methylation in DNA
g
miR-181a2 methylation in DNA

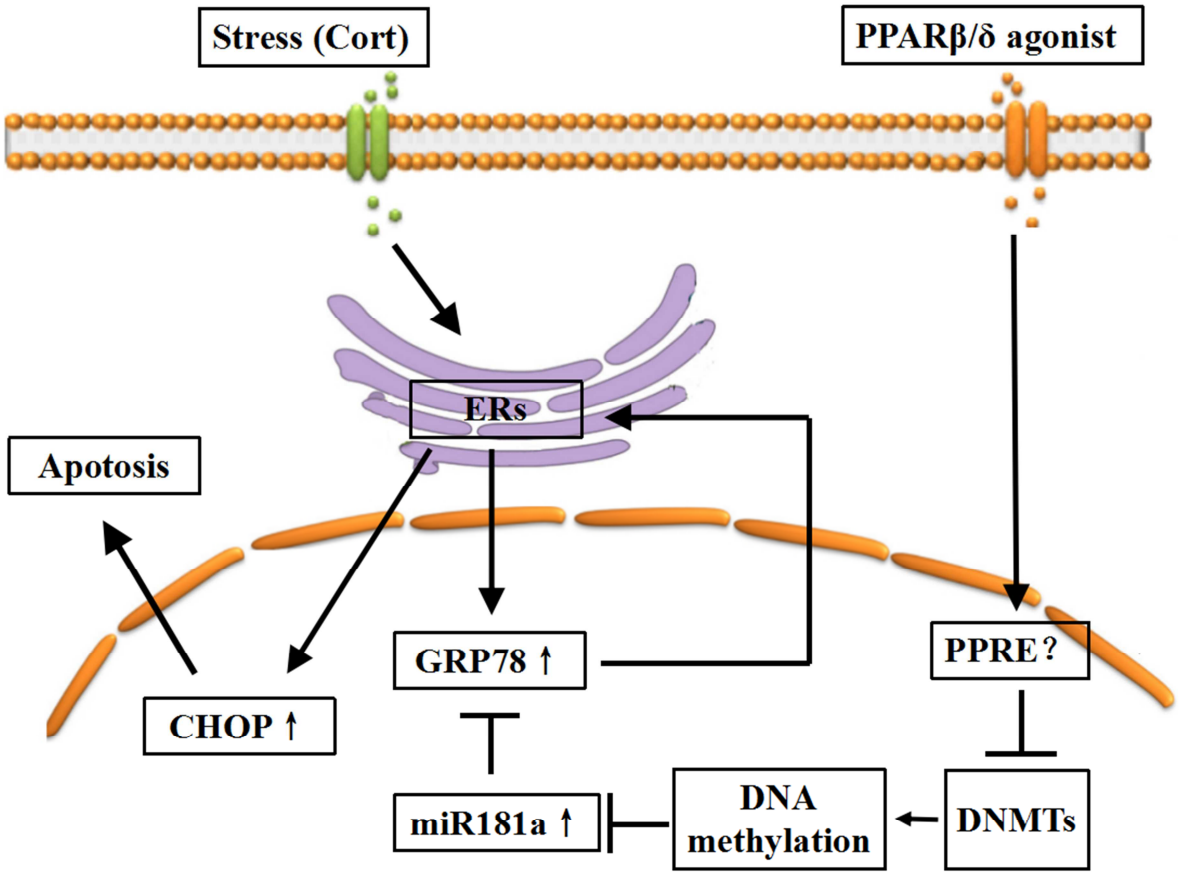

Highlights

1. PPARβ/δ is the dominant subtype expressed in the primary cultured astrocytes
2. PPARβ/δ activation protects against corticosterone-induced astrocyte damage
3. PPARβ/δ activation protects against ER stress-induced apoptosis of astrocytes
4. PPARβ/δ activation up-regulates miR-181a levels in astrocytes
5. PPARβ/δ activation inhibits Dnmts and decreases CpG island methylation of MiR-181a1